Geochemistry, Geophysics, Geosystems®

RESEARCH ARTICLE
10.1029/2021GC010017

Special Section:
Carbon degassing through volcanoes and active tectonic regions

Active Degassing of Deeply Sourced Fluids in Central Europe: New Evidences From a Geochemical Study in Serbia

P. Randazzo[1], A. Caracausi[2], A. Aiuppa[1], C. Cardellini[3,4], G. Chiodini[4], W. D'Alessandro[2], L. Li Vigni[1], P. Papic[5], G. Marinkovic[6], and A. Ionescu[3,7,8]

[1]Dipartimento di Scienze della Terra e del Mare, Università di Palermo, Palermo, Italy, [2]Istituto Nazionale di Geofisica e Vulcanologia, Sezione di Palermo, Palermo, Italy, [3]Dipartimento didi Fisica e Geologia, Università di Perugia, Università degli Studi di Perugia, Perugia, Italy, [4]Istituto Nazionale di Geofisica e Vulcanologia, Sezione di Bologna, Bologna, Italy, [5]Faculty of Mining and Geology, University of Belgrade, Beograd, Serbia, [6]Geological Survey of Serbia, Belgrade, Serbia, [7]Faculty of Environmental Science and Engineering, ISUMADECIP, Babes-Bolyai University, Cluj-Napoca, Romania, [8]Department of Geology, Babes-Bolyai University, Cluj-Napoca, Romania

Abstract We report on the results of an extensive geochemical survey of fluids released in the Vardar zone (central-western Serbia), a mega-suture zone at the boundary between Eurasia and Africa plates. Thirty-one bubbling gas samples are investigated for their chemical and isotopic compositions (He, C, Ar) and cluster into three distinct groups (CO_2-dominated, N_2-dominated, and CH_4-dominated) based on the dominant gas species. The measured He isotope ratios range from 0.08 to 1.19 Ra (where Ra is the atmospheric ratio), and reveal for the first time the presence of a minor (<20%) but detectable regional mantle-derived component in Serbia. $\delta^{13}C$ values range from −20.2‰ to −0.1‰ (versus PDB), with the more negative compositions observed in N_2-dominated samples. The carbon-helium relationship indicates that these negative $\delta^{13}C$ compositions could be due to isotopic fractionation processes during CO_2 dissolution into groundwater. In contrast, CO_2-rich samples reflect mixing between crustal and mantle-derived CO_2. Our estimated mantle-derived He flux (9.0×10^9 atoms m^{-2} s^{-1}) is up to 2 orders of magnitude higher than the typical fluxes in stable continental areas, suggesting a structural/tectonic setting favoring the migration of deep-mantle fluids through the crust.

Key Points:

- Chemical and isotopic composition of natural gas manifestations along the Serbian Vardar zone are controlled by mixing processes and fraction during water-gas-rock interactions in shallow crustal layers
- Mantle-derived He flux of 2 orders of magnitude higher than normally found in stable continental areas are estimated
- Mantle volatiles and heat are sourced directly from the mantle supporting the asthenosphere up-rise and delamination processes at the mantle-crust boundary recognized in the studied area

Supporting Information:

Supporting Information may be found in the online version of this article.

Correspondence to:

P. Randazzo,
paolo.randazzo@unipa.it

Citation:

Randazzo, P., Caracausi, A., Aiuppa, A., Cardellini, C., Chiodini, G., D'Alessandro, W., et al. (2021). Active degassing of deeply sourced fluids in central Europe: New evidences from a geochemical study in Serbia. *Geochemistry, Geophysics, Geosystems*, *22*, e2021GC010017. https://doi.org/10.1029/2021GC010017

Received 21 OCT 2021

1. Introduction

Recognizing and identifying the transfer of mantle-derived fluids (e.g., CO_2, N_2, noble gases) in continental regions is critical for investigating the processes that shape the deep and shallow Earth's evolution, such as subduction, volcanism, natural degassing, active tectonics, and earthquakes (e.g., Ballentine et al., 2001; Broadley et al., 2020; Caracausi & Sulli, 2019; Caracausi et al., 2013; Chiodini et al., 2020; Holland & Gilfillan, 2013; Kennedy & Van Soest, 2007; Labidi et al., 2020; Lowenstern et al., 2014; O'Nions & Oxburgh, 1988; Torgersen, 1993). During the last four decades, the migration and surface discharge of deep-mantle volatiles has been verified in many crustal segments, including western-central Europe (e.g., Brauer et al., 2013; Carreira et al., 2009; Mamyrin & Tolstikhin, 1984; Minissale, 2000). New efforts are currently undertaken to extend such studies in central-eastern Europe, in the attempt to (a) understand natural degassing in active tectonic regions (e.g., Etiope et al., 2003, 2004; Frunzeti, 2013; Ionescu et al., 2017; Italiano et al., 2017; Kis et al., 2017; Sarbu et al., 2018; Vaselli et al., 2002), (b) investigate the possible presence of magma at depth below "quiescent" volcanoes (e.g., Kis et al., 2019), and (c) assess the role of fluids in seismogenetic processes (e.g., Baciu et al., 2007; Bräuer et al., 2004, 2005, 2008). Large-scale outgassing of mantle-derived fluids has been recognized in different European volcanic regions that last erupted thousands of years ago (e.g., Eger rift, Czech Republic; Eifel, Germany; Carpathians, Romania; Pannonian basin; Aeschbach-Hertig et al., 1996; Ballentine et al., 1991; Bräuer et al., 2013, 2016; Kis et al., 2017, 2019; Palcsu et al., 2014; Sherwood Lollar et al., 1997; Szöcs et al., 2013). Further to the south, in Greece and Turkey, a link between fluid release (with mantle-derived components), tectonic setting, and seismicity has been demonstrated, in both volcanic and nonvolcanic areas (e.g., D'Alessandro et al., 2020; Daskalopoulou et al., 2019; De Leeuw et al., 2010; Dogan et al., 2009; Italiano et al., 2013; Mutlu et al., 2008; Rizzo et al., 2018; Shimizu et al., 2005).

The Serbian segment of the seismically active central-western Balkan Peninsula (Marović et al., 2002) is sited at the suture zone between African (Adria) and European plate. The area is characterized by delamination and sinking of the Adria mantle lithosphere under the north-western and southern Dinarides, with hotter mantle materials filling the space left by the sinking slabs (e.g., Belinić et al., 2021). Serbia also exhibits high regional heat flow (up to 130 mW/m^2) and geothermal energy potential (Doljak & Glavonjić, 2016; Horwarth et al., 2015). Previous work in the central-western Balkan Peninsula has found several natural gas manifestations and gas-rich thermal waters (e.g., Burić et al., 2016; Rosca et al., 2016; Todorović et al., 2016). However, the source of these gases, and the geological/tectonic controls on their migration through the crust, remain uncharacterized.

Here, we report on the results of a geochemical survey (carried out in autumn 2019) aimed at investigating the origin (e.g., atmospheric versus crustal versus mantle-sourced) of the volatiles outgassed in Serbia. We also attempt at a better characterization of the processes that control the chemistry of the fluids during their storage in, and transit through, the crust. Our study contributes to filling a knowledge gap on the nature of fluids circulating in this sector of Europe, and helps better reconstructing the complex geodynamic of the area.

2. Geological Setting

The sector of the Vardar zone in Serbia (south eastern Europe, SEE) is part of the mega-suture stretching along the entire Balkan Peninsula (e.g., Cvetković et al., 2016). Its present-day geological setting is the result of a complex geodynamic and tectonic evolution over the last ~200 Ma (from the middle Mesozoic to the present) that progressively involved subduction, continental collision, and finally lithospheric extension (e.g., Belinic et al., 2021; Cvetković et al., 2004). The engine of the regional geodynamic evolution is the interaction between Eurasian (Europe) and Gondwana (Africa) continental plates (Cvetković et al., 2016). More in detail, Serbia is part of the orogenic system composed by the Alpine, Carpathian, and Dinaride belts (e.g., Marović et al., 2007; Schmidt et al., 2008, 2019) and its territory can be divided into distinct tectonic units: (a) the Pannonian basin (northern part), (b) the Dinaric Alps (central-western part), (c) the Vardar zone, divided in East and West zones (the study area, Figure 1), (d) the Serbian-Macedonian Massif, a belt stretching in north-south direction into north-western Macedonia and northern Greece, (e) the Carpatho-Balkan Region (eastern part), and (f) the Dacia basin (Bazylev et al., 2009; Cvetković et al., 2004; Jelenković et al., 2008; Moores & Fairbridge, 1997).

In the study area, volcanism has recurrently insisted over the last ~200 Ma (e.g., Cvetković et al., 2016; Zelić et al., 2010), and includes alkaline magmatism during the middle to late Triassic rifting stage (Bortolotti et al., 2008), intrusive magmatic activity with calk-alkaline granitoids in the Late Jurassic-Miocene, and granitoid products in the early Eocene-late Oligocene (Pamić et al., 2002; Saric et al., 2009). Since the Oligocene, widespread volcanism occurred throughout SEE, associated to the formation of a variety of volcanic landforms. Volcanism in Serbia concentrated along an NW-SE-trending belt (Cvetković et al., 2016), with the youngest volcanic activity pulse dating 16.8-8.6 Ma (Zelić et al., 2010, and reference therein). Currently, in the region, there are widespread outcrops of volcanic rocks, ranging in composition from andesites to basanites (upper Cretaceous-middle Paleogene), shoshonites and high-K calc-alkaline series with occurrence of lamproites (Cvetković et al., 2000; Djordjević, 2005; Pamić, 1997; Prelević et al., 2005; Zelić et al., 2010).

The final stage of the regional geodynamic evolution involved an extensional phase of lithospheric thinning (Cvetković et al., 2016) that culminates in the Pannonian Basin and the Serbian-Macedonian Massif (40–50 km of lithospheric crust) and is associated to an asthenosphere up-rise (Cvetković et al., 2016; Milivojević, 1993). The heat flow distribution in the Pannonian basin is consequently high (from 50 to 130 mW/m^2), and the highest values are observed in the Great Hungarian Plain, the Pannonian part of Serbia (Vojvodina) including its continuation into the Vardar zone (Horvath et al., 2015; Lenkey et al., 2002).

The region is characterized by active seismicity with earthquake magnitudes up to 6.5 and hypocenters down to 20–30-km depth (http://www.seismo.gov.rs/Seizmicnost/Katalog-zemljotresa.pdf) and this depth coincides with the regional crust-mantle boundary (Marović et al., 2007; Metois et al., 2015).

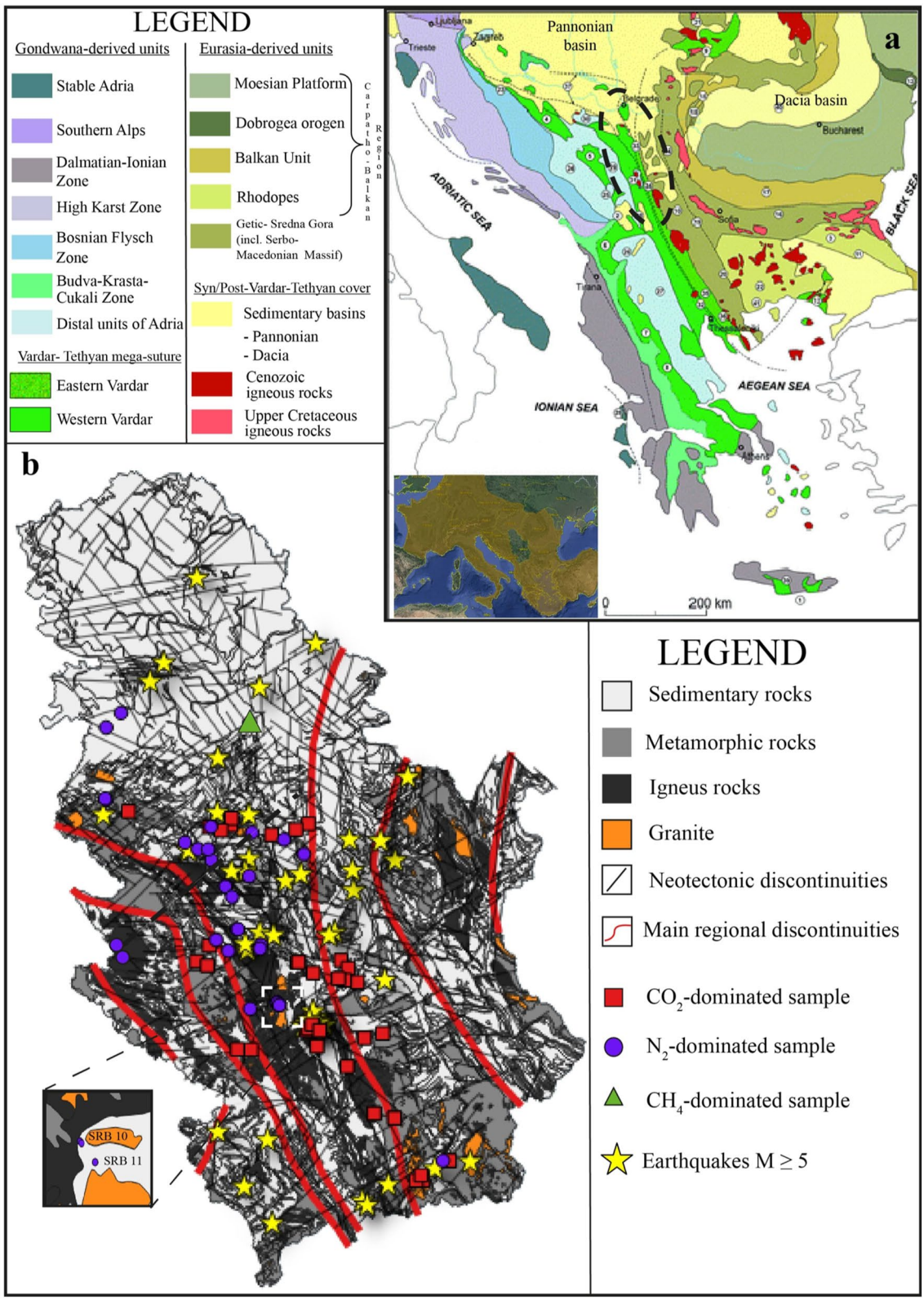

Figure 1. (a) Simplified geological sketch map of south eastern Europe with the main tectonic units (for detailed information see Cvetkovic et al. [2016]). The studied area is highlighted by the dashed ellipse on the map. Small inset at the bottom left indicates the European areas in which geochemical studies on natural degassing have been conducted (shaded yellow area); (b) geological map of Serbia with sample locations, main regional faults (red), and neotectonic faults (black). The small inset is a zoom on the area in which a sample with lowest R/Ra has been collected in correspondence to a granitoid intrusion.

3. Materials and Methods

Thirty-one bubbling gas samples were collected from north to south in the central and western sectors of Serbia (Figure 1b). The bubbling gases were sampled by using an inverted funnel that was positioned above the bubbles, so the gases fluxed through a two valves glass or steel bottle to avoid air contamination. Once the bottles had been flushed with an amount of gas at least tens of times the volume of the bottles (20–30 cc) the valves were closed to trap the gases into the bottles. All chemical and isotopic analyses were carried out at the laboratories of the INGV-Palermo within 1 month from the sampling in order to prevent isotopic fractionation due to storage of gases. Water temperature and pH were measured in the field by using a portable multiparameter instrument (WTW Multi 350i), which was previously calibrated using standard solutions (Table 1). The chemical composition of the gases was analyzed by an Agilent 7890B gas chromatograph using Ar as carrier gas, and equipped with 4-m Carbosieve S II and PoraPlot-U columns. A thermal conductivity detector (TCD) was used to measure the concentrations of O_2, N_2, and CO_2, while a flame ionization detector (FID) was used for CH_4. Analytical errors of the measured concentrations are always within 5%.

The $^{13}C/^{12}C$ ratios of CO_2 (expressed as $\delta^{13}C\text{-}CO_2$ in ‰ versus the V-PDB standard) were measured with a Finnigan Delta S mass spectrometer after purification of the gas mixture by standard procedures using cryogenic traps with precision of ±0.1‰. He isotopes were analyzed using a static vacuum mass spectrometer (GVI Helix SFT), using a double collector in order to detect ^3He and ^4He ion beams simultaneously (precision for isotopic ratio within ±0.5%). The $^3He/^4He$ ratio was determined by measuring ^3He in an electron multiplier detector and ^4He in an axial Faraday detector. ^{20}Ne was measured with a multicollector Thermo-Helix MC Plus mass spectrometer. Helium isotope compositions are expressed as R/Ra, normalizing the $^3He/^4He$ ratio of the sample against the atmospheric $^3He/^4He$ ratio ($Ra = 1.386 \times 10^{-6}$; Ozima & Podosek, 2002). The Ar concentrations and its isotope compositions (^{40}Ar, ^{38}Ar, and ^{36}Ar) were analyzed by multicollector Helix MC-GVI mass spectrometer with analytical uncertainty (1σ) for single $^{40}Ar/^{36}Ar$ measurements of <0.1%.

4. Results

The chemical composition of the sampled gases, together with the isotopic composition of He, Ar, and C (CO_2), are presented in Table 1.

On the base of their chemical compositions, the studied gases are subdivided into three different groups: CO_2-dominated (CO_2 > 50%), N_2-dominated (N_2 > 50%), and CH_4-dominated (this includes only sample SRB31, being methane-rich: 87%) (Table 1). CO_2-dominated and N_2-dominated samples have CH_4 concentrations ranging from 0.02% to 19. Ar and O_2 concentrations are typically ≤1% (Table 1), and He and Ne are present in trace amounts (ppmv). The CH_4-dominated sample has a CO_2 concentration of 0.51% and N_2 of 11%. Also, for this sample, the O_2 and Ar concentration are very low (<1%) with He and Ne present in trace (37.3 and 0.24 ppmv). CO_2 and N_2 exhibit a negative correlation, as implied by their being the two dominant gas species (Figure 2). Only the CH_4-rich sample, and two other N_2-dominated samples (10.1–51.6% of N_2) that are bubbling gases from hyperalkaline waters (pH from 11.6 to 12.2) depart from a pure CO_2-pure N_2 mixing line. Gases in hyperalkaline waters have high amount of H_2 (85% and 34%) and very low CO_2 amounts (<0.15%).

The $\delta^{13}C_{CO2}$ values vary from −20.2‰ to −0.1‰ (Table 1). The N_2-dominated gases exhibit the lowest $\delta^{13}C\text{-}_{CO2}$ values, especially those with CO_2 <3% that plot in the field of biogenic CO_2 (Figure 3). The CO_2-C isotopic compositions of bubbling gases in hyperalkaline waters also plot in the same biogenic field (Figure 3).

The He isotopic ratios, expressed as R/Ra, vary from 0.08 to 1.2 Ra, and the N_2-dominated gases have the lowest He isotopic ratios (Figure 4). The $^4He/^{20}Ne$ ratios mostly range from 13 to 1,300, and are much higher than the atmospheric ratio (0.318; Ozima & Podosek, 2002), indicating a low air He contribution to the sampled gases. On the contrary, the two hyperalkaline samples have $^4He/^{20}Ne$ values of 0.53 and 0.59 indicating a dominant atmospheric component.

Geochemistry, Geophysics, Geosystems

10.1029/2021GC010017

Table 1
Location, Geochemical, and Isotopic Composition of the Sample

Name	Code	Coordinates E	Coordinates N	Date	pH	T(°C)	CO_2(%)	N_2 (%)	O_2 (%)	CH_4 (%)	H_2 (ppm)	He (ppm)	Ne (ppm)	Ar (ppm)	R/Ra	He/Ne	$\delta^{13}C(CO_2)$ ‰ (versus V-PDB)	$CO_2/^3He$	$^{40}Ar/^{36}Ar$	Atm %	Mantle %
Vranjska Banja	SRB1	42.5452	22.0064	06/11/2019	6.5	90	44.14	54.27	0.26	1.72	802	1,013	8.81	6,120	0.31	115	−4.7	1.00E+09	298.6	0.25	5.04
Suva Cesma	SRB5	43.2345	21.5144	07/11/2019	6.36	21.1	43.52	55.90	0.06	0.13	—	1,068	9.36	6,150	0.30	114	−9.0	9.80E+08	297.4	0.26	4.88
Vica	SRB6	43.2094	21.3810	07/11/2019	7.4	14.6	22.40	73.45	0.39	2.31	—	5,819	4.38	5,617	0.28	1,329	−10.9	9.76E+07	307.5	0	4.59
Josaniska Banja	SRB10	43.4001	20.7353	08/11/2019	8.3	73.1	0.13	98.28	0.11	0.19	11	862	12.68	13,500	0.10	68.0	−17.7	1.10E+07	296.9	0.45	1.57
Josaniska Banja	SRB11	43.3869	20.7528	08/11/2019	8.3	71.5	0.02	97.30	0.32	0.39	6	360	11.83	15,800	0.08	30.4	−16.2	5.89E+06	297.1	1.02	1.14
Mokra Gora	SRB16/A	43.7936	19.5253	10/11/2019	12.23	—	0.10	10.43	0.09	7.14	816,200	—	—	2,350	—	—	−14.3	—	—	—	—
Mokra Gora	SRB16/B	43.7936	19.5253	10/11/2019	12.23	15.9	0.15	10.16	0.08	5.21	854,100	0.95	1.79	2,190	0.70	0.53	−17.1	1.61E+09	295.2	59.98	1.64
Ribnica	SRB17/A	43.7035	19.5788	10/11/2019	11.66	15.1	0.003	51.63	0.06	14.68	340,500	4.32	7.32	7,280	0.57	0.59	—	9.31E+06	296.7	53.88	0.51
Ribnica	SRB17/B	43.7033	19.5790	10/11/2019	11.66	—	0.003	51.79	0.19	15.73	323,600	—	—	6,300	—	—	—	—	—	—	—
Petnica	SRB21	44.2454	19.9357	11/11/2019	7.11	14.9	2.03	93.07	3.76	0.02	—	7	—	8,640	—	—	−19.7	—	—	—	—
Bogatic	SRB29	44.8709	19.4803	13/11/2019	6.3	78	25.34	55.93	0.29	19.06	65	401	6.85	10,800	0.24	58.5	−5.2	1.91E+09	295.1	0.52	3.85
Savinac 2	SRB30	44.0257	20.3856	13/11/2019	7.1	19.4	2.53	92.38	0.0004	0.04	—	194	—	9,860	—	—	−20.2	—	—	—	—
Mataruska Banja	SRB12	43.6901	20.6113	09/11/2019	6.3	50	32.25	65.65	0.67	1.56	—	1,066	6.37	7,970	0.91	167	−6.4	2.37E+08	298.0	0.17	14.89
Ovca	SRB31	44.8908	20.5349	13/11/2019	7.57	19.4	0.51	11.07	0.07	87.66	3	37.3	0.24	509	0.89	154	−9.2	1.10E+08	348.8	0.18	14.56
Tulare	SRB3	42.8019	21.4518	06/11/2019	6.8	34.5	95.78	4.37	0.45	0.01	—	62.8	0.13	231	0.57	466	−4.5	1.90E+10	305.5	0.05	9.34
Sijarinska Banja	SRB4	42.7764	21.6008	06/11/2019	6.43	58	99.88	0.89	0.22	0.03	—	2.34	0.06	32	0.80	38.7	−4.6	3.83E+11	299.1	0.8	12.98
Kursumlijska Banja	SRB7	43.0570	21.2528	07/11/2019	6.56	68	93.59	5.58	0.18	0.41	—	66.0	0.41	594	0.28	161	−5.3	3.63E+10	298.7	0.18	4.56
Lukoska Banja	SRB8/A	43.1645	21.0307	08/11/2019	6.7	41.7	90.50	8.79	0.3	0.13	—	59	—	—	—	—	−2.9	—	—	—	—
Lukoska Banja	SRB8/B	43.1645	21.0307	08/11/2019	6.09	54	91.71	5.82	0.18	0.08	—	72.6	0.51	873	0.73	142	−2.6	1.24E+10	297.1	0.2	11.93
Lukoska Banja	SRB8/C	43.1644	21.0323	08/11/2019	6.23	70	91.63	7.77	0.37	0.28	—	85	—	846	—	—	−2.5	—	—	—	—
Zarevo	SRB9	43.2824	20.9938	08/11/2019	5.88	12.9	94.34	3.93	0.07	1.23	—	50.9	0.39	652	0.53	130	−0.1	2.50E+10	303.3	0.22	8.65
Vrnjacka Banja	SRB13	43.6176	20.8863	09/11/2019	6.2	34.5	91.95	5.51	0.10	1.60	—	106	0.38	619	1.00	278	−2.4	6.19E+09	300.3	0.09	16.38
Lomnicki Kiseljak	SRB14	43.5110	21.3281	09/11/2019	6.5	16.8	82.59	14.77	1.89	0.02	—	318	1.10	1,280	0.53	290	−5.0	3.51E+09	306.4	0.09	8.67
Cibutkovica	SRB23	44.3380	20.2381	12/11/2019	6.1	20.7	96.85	1.52	0.07	1.47	14	29.8	0.18	181	0.85	161	−4.5	2.74E+10	300.9	0.18	13.91
Krusevica	SRB24	44.3473	20.3960	12/11/2019	6.3	21.4	96.79	1.78	0.35	0.90	1.7	2.92	0.23	250	0.95	12.7	−5.2	2.49E+11	295.1	2.48	15.17
Rudovci	SRB25	44.3835	20.4000	12/11/2019	6.5	17.2	92.89	4.72	0.22	2.52	—	181	0.23	354	1.19	779	−6.0	3.07E+09	312.1	0.02	19.51
Rudovci	SRB25/A	44.3835	20.4000	12/11/2019	—	—	98.08	1.31	0.07	1.08	—	—	—	—	—	—	−6.1	—	—	—	—
Vozd Voda	SRB26	44.2963	20.6955	12/11/2019	6.6	19.8	58.35	37.67	0.06	3.95	—	586	1.37	1,830	0.56	427	−8.8	1.28E+09	308.7	0.05	9.17
Cerovac	SRB27	44.3244	20.8747	12/11/2019	6.3	19.5	97.04	1.35	0.06	0.80	—	6.50	0.20	180	0.51	33.0	−6.3	2.08E+11	301.5	0.94	8.21
Smederevska Palanka	SRB28	44.3542	20.9674	12/11/2019	6.2	20.7	98.10	0.70	0.07	2.56	—	2.56	0.08	116	0.52	31.4	−7.3	5.26E+11	296.8	0.99	8.36
Ljiljance/ Bujanovac	SRB2	42.4387	21.8119	06/11/2019	6.47	18.7	95.06	6.08	0.08	0.003	—	108	0.42	680	0.34	259	−5.6	1.87E+10	298.6	0.1	5.56

Note. Major elements in %, H_2 and noble gases in ppm. $\delta^{13}C$ of CO_2 in ‰ versus V-PBD. Percentage of atmosphere (Atm) and mantle calculated following Sano et al. (1985).

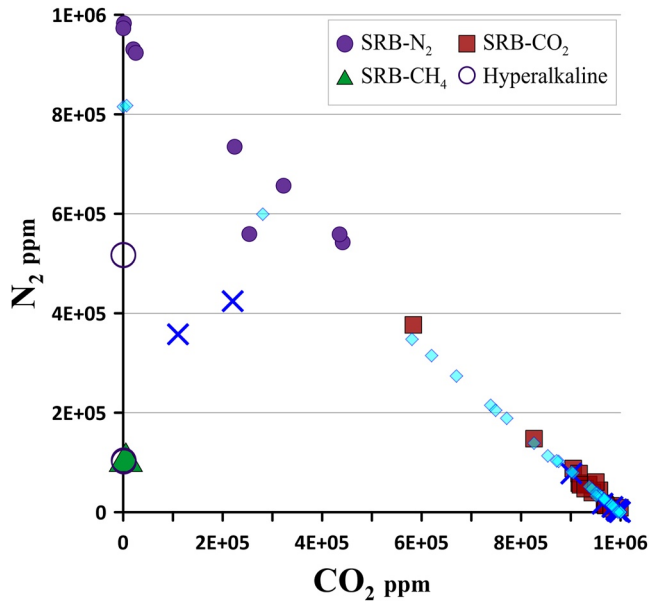

Figure 2. A scatter plot of N_2 versus CO_2 concentrations (in ppm) in Serbian gases. See legend for symbols of three groups of fluids in the studied area. Purple open circles that along the *y* axis are two samples of bubbling gases in hyperalkaline water. The light blue diamonds and the dark blue crosses depict data from some central and eastern Europe areas (Eger rift; Weinlich et al., 1999) and from the Austria/Slovenia border, Pannonian basin (Bräuer et al., 2016).

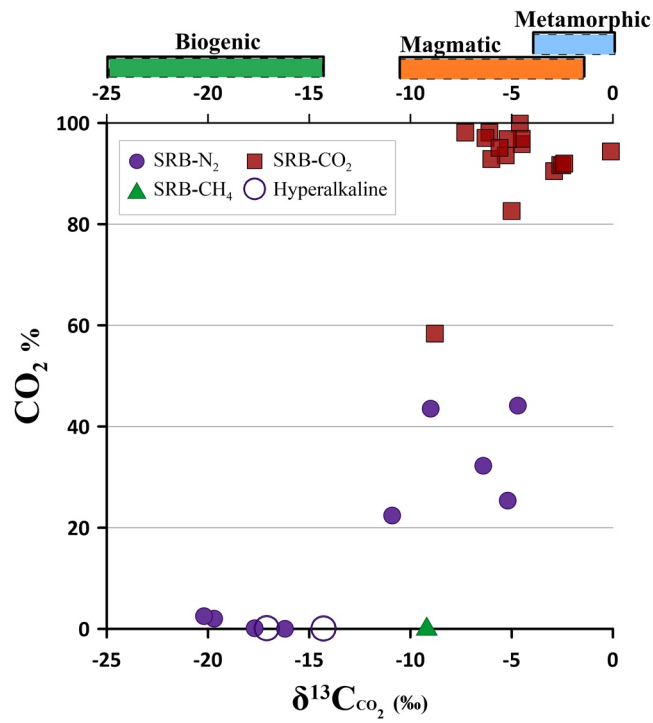

Figure 3. A scatter plot of CO_2 concentrations versus CO_2 carbon isotopic composition ($\delta^{13}C$). N_2-dominated gases (especially those with CO_2 <3%) exhibit the lowest $\delta^{13}C_{CO2}$ values, falling in the field of the biogenic CO_2 (green bar). Gases from hyperalkaline waters also plot in the same field of biogenic CO_2. CO_2-rich samples have more positive carbon isotopic compositions, falling within the magmatic (orange) and metamorphic (blue) fields. The three colored boxes indicate the typical $\delta^{13}C$ ranges for the three different sources: green = biogenic, orange = magmatic, blue = metamorphic. Note the overlap between the two field (magmatic-metamorphic) at ~4‰ (from Holland and Gilfillan [2013]).

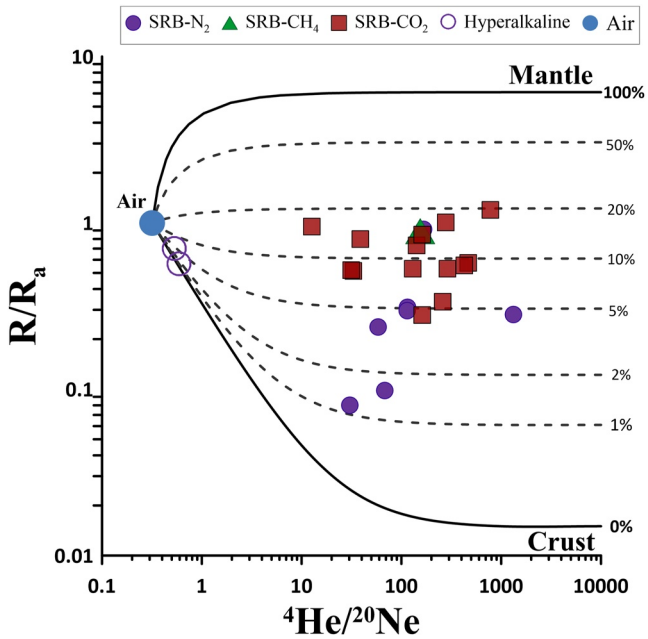

Figure 4. $^{3}He/^{4}He$ ratios (expressed as R/Ra) versus $^{4}He/^{20}Ne$ ratios. CO_2-dominated samples (red squares) exhibit the ^{3}He-richest isotope signatures (corresponding to mantle He contributions of 5–20%), whereas N_2-dominated gases (purple circles) extend to more radiogenic values (i.e., crustal) with mantle He contributions up to 5%. For these samples only SRB12 show higher mantle He contribution like CO_2-dominated samples. Samples from the hyperalkaline waters have the lowest $^{4}He/^{20}Ne$ ratios, reflecting an atmospheric derivation.

5. Discussion

He in natural fluids from tectonically active regions is typically interpreted as originating from three distinct sources: the mantle, the crust, and air (e.g., Burnard et al., 2013; O'Nions & Oxburgh, 1988; Sano et al., 1997). These three sources are characterized by distinct He isotopic signatures: (a) 6.1 ± 0.9 Ra, for the European Subcontinental Lithospheric Mantle, ESCLM (Gautheron & Moreira, 2002); (b) 0.01–0.02 Ra, for pure crustal fluids dominated by radiogenic ^{4}He produced by U and Th decay (Ballentine & Burnard, 2002); (c) 1 Ra, for air (Ozima & Podosek, 2002). $^{4}He/^{20}Ne$ ratios are >1,000 for crust and mantle and 0.318 for air respectively (Sano et al., 1985). Because of these different end-member compositions, He isotopes in natural fluids, coupled with their $^{4}He/^{20}Ne$ ratios, can be used to resolve the relative He contributions from the three sources (e.g., Caracausi & Sulli, 2019; Sano & Wakita, 1985; Sano et al., 1997, and references therein). Using the approach proposed in Sano et al. (1997), and assuming that all ^{20}Ne is atmospheric, we estimate low atmospheric contributions (<3%, Table 1) for all samples, except those collected from the hyperalkaline waters, and mantle helium fractions of 1% to ~20%, with the highest fractions calculated for the CO_2-dominated samples (Figure 4).

It is interesting to note that the two N_2-rich samples (SRB10 and SRB11) with the lowest He isotopic signatures (R/Ra < 0.1; mantle component ~1%) have been collected nearby two large granite intrusions (see inset in Figure 1) that are characterized by high U and Th concentrations (of, respectively, 563 and 270 ppm) (Schefer et al., 2011). Hence, it is reasonable that these low He isotopic ratios reflect the high radiogenic ^{4}He production in the U-Th-rich lithologies.

5.1. Insights From $CO_2/^{3}He$ Ratios

Additional insights into volatile sources and sinks, and into the processes occurring during (a) the migration of fluids through the crust and (b) their storage in shallow crustal layers can be derived from a joint analysis and interpretation of He and carbon isotopic signatures (e.g., Barry et al., 2020; Holland & Gilfillan, 2013). Our study highlights that natural gases in the Vardar zone of Serbia are dominated by either CO_2 or N_2 (Figure 2) and are characterized by a significant spread of $\delta^{13}C$ compositions (Figure 3) and R/Ra ratios (Figure 4) that could reflect a multiplicity of gas sources involved. ^{3}He in natural fluids is mainly primordial and sourced from the mantle. Thus, combining CO_2 and ^{3}He (into the $CO_2/^{3}He$ ratio) allows evaluating enrichments or depletions relative to a mantle-like signature (Figure 5).

However, in continental environments, the lithospheric mantle often brings record of heterogeneities caused by metasomatizing events (Rizzo et al., 2018) that can lead to C enrichment ($CO_2/^{3}He$ ratio of 7×10^{9}) with respect to the MORB ($1.5–2 \times 10^{9}$; Marty et al., 2020). The European Subcontinental Lithospheric Mantle (ESCLM) is thought to be also isotopically heavier than the MORB ($\delta^{13}C_{CO2}$ of MORB from −8‰ to −4‰; Bräuer et al., 2016; Rizzo et al., 2018, and reference therein), so that we assume here a $CO_2/^{3}He$ ratio of $2–7 \times 10^{9}$ and $\delta^{13}C$ of −3.5‰ (Bräuer et al., 2016) for the local mantle source.

Our CO_2-rich and N_2-rich fluids are characterized by distinct $CO_2/^{3}He$ ratios that are, respectively, higher (up to 5.26×10^{11}) and lower (as low as 5.89×10^{6}) than the above defined mantle range (Figure 5). In tandem with gas samples from nearby regions (Eger rift, Weinlich et al., 1999; Austria/Slovenia border region, Pannonian basin; Bräuer et al., 2016), our samples identify a continuous trend from (a) a CO_2-rich, high $CO_2/^{3}He$ ratio end-member, and (b) a ^{4}He-^{20}Ne-rich, low $CO_2/^{3}He$ ratio end-member (Figures 5a–5c). The high $CO_2/^{3}He$ ratios ($10^{12}–10^{14}$) of most CO_2-rich crustal continental gases are commonly interpreted (Sano & Marty, 1995; Sherwood Lollar et al., 1997) to result from decarbonation reaction and biological processes in the crust that produce a CO_2-rich, ^{3}He-free gas. We thus propose that the CO_2-dominated gases are mix-

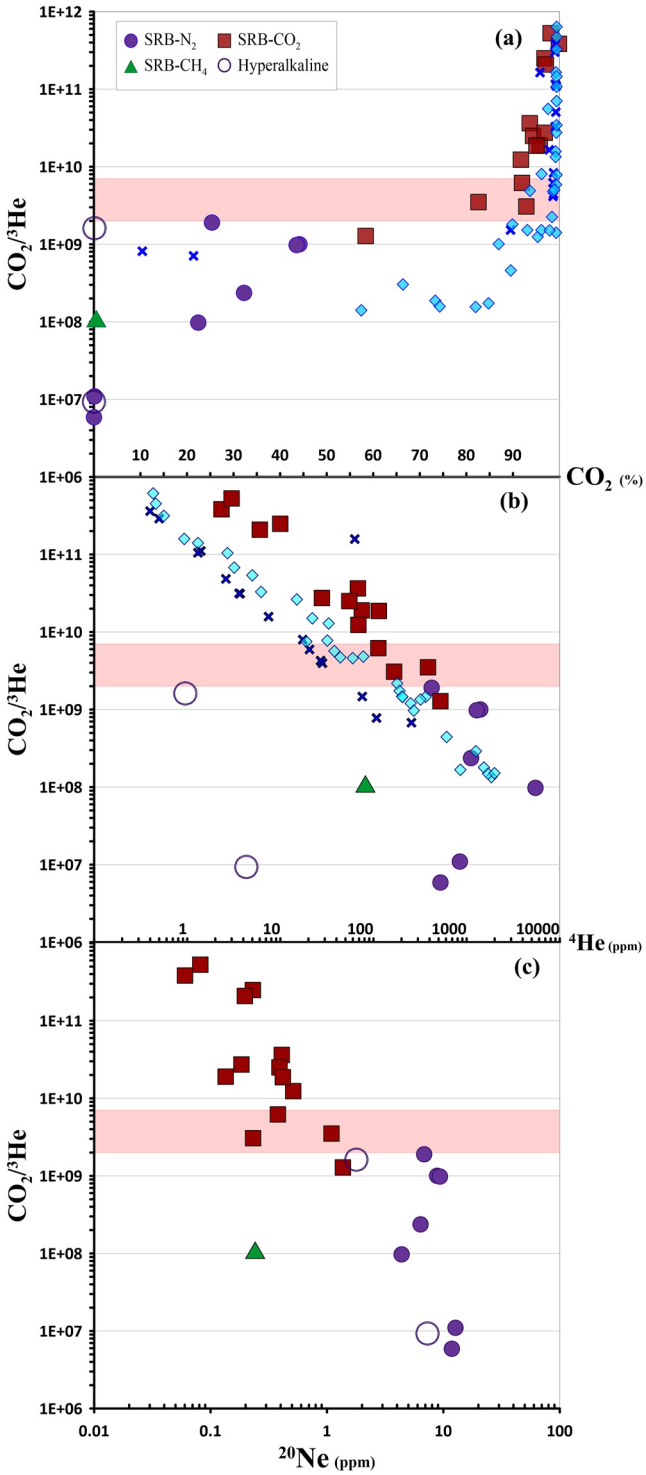

Figure 5. $CO_2/^3He$ ratios versus (a) CO_2, (b) ^4He, and (c) ^{20}Ne concentrations. The panel shows a trend from CO_2-rich, high $CO_2/^3He$ (low in He and Ne) samples to He-Ne-rich, low $CO_2/^3He$ ratio samples. The SCLM range is given by the shaded area ($CO_2/^3He = 2–7 \times 10^9$; Bräuer et al., 2016; Marty et al., 2020). Data for other central and eastern Europe areas follow the same trend (dark blue crosses, Bräuer et al., 2016; light blue diamonds, Weinlich et al., 1999).

tures of CO_2-rich crustal gas with a 5–20% mantle-derived component (Figure 4). This is additionally supported by Figure 6, in which the CO_2-rich samples fall along hypothetical mixing curves between a SCLM pole and a set of hypothetical crustal end-members with same radiogenic R/Ra ratio but different $CO_2/^3He$ ratios.

Moreover, a crustal (limestone + organic-biogenic) carbon addition to a SCLM-like gas is suggested by the $\delta^{13}C$ versus $CO_2/^3He$ ratio plot of Figure 7.

Solid gray lines show mixing between three end-member: mantle ($CO_2/^3He = 2–7 \times 10^9$, $\delta^{13}C = -3.5‰$; Bräuer et al., 2016; Rizzo et al., 2018), limestone ($CO_2/^3He = 10^{13}$, $\delta^{13}C = 0‰$), and sediment ($CO_2/^3He = 10^{13}$, $\delta^{13}C = -30‰$) after Sano and Marty (1995).

Interpreting the N_2-dominated samples is less straightforward. However, except for sample SRB12, He in all the investigated N_2-dominated gases is minimally contributed by the mantle (<5%; Figure 4) and by atmosphere (Figure 4). Furthermore, these samples exhibit the highest ^4He and ^{20}Ne contents (Figures 5b and 5c), and the lowest $CO_2/^3He$ ratios and He isotopic signatures (Figure 6). Although there is no a priori reason to expect a correlation between ^4He and ^{20}Ne with the $CO_2/^3He$ ratio, such a correlation has been found regionally in natural gases (Ballentine et al., 2002; Gilfillan et al., 2009). ^4He is constantly produced in the subsurface by the radiogenic decay of U, Th, while ^{20}Ne enters subsurface groundwater systems as a component of air-saturated meteoric water (Ballentine & Sherwood Lollar, 2002). This atmospheric component can then be transferred to natural fluids in crustal layers, interacting with the groundwater that are able to trap the air component together with large amount of radiogenic volatiles (e.g., ^4He) produced over time into the crust and degassing through it (e.g., Ballentine et al., 2002). Previous studies indicated that such correlations are the result of ^4He accumulating in the groundwater which also contains atmospheric-derived ^{20}Ne, and subsequent quantitative partitioning of both ^4He and ^{20}Ne into the gas phase due to fractionation events, probably in the groundwater (e.g., Gilfillan et al., 2008). It is worth noting that gases from gas-fields from central and eastern Europe (e.g., Eger rift, Austria/Slovenia border region, Pannonian basin) fit with similar CO_2-N_2-He concentration arrays (e.g., Bräuer et al., 2016; Weinlich et al., 1999), supporting the recurrence of solubility-dependent volatile fractionation.

The low CO_2 concentrations and low $CO_2/^3He$ ratios in the N_2-dominated gases (Figures 4–6), combined with their more negative ^{13}C-compositions (Figure 7), imply some mechanism of CO_2 removal during gas-water-rock interactions. During their migration through the crust, volatiles can interact with groundwater and, due to its high solubility, CO_2 dissolves preferentially in water relative to He (in the range of temperature up to 90 °C: CO_2 solubility > He solubility; Ballentine et al., 2002; Clever et al., 1979; Gilfillan et al., 2009; Scharlin et al., 1996). Furthermore, groundwater can also precipitate carbonate minerals, additionally modifying the dissolved carbonate equilibria (Barry et al., 2020; Gillfillan et al., 2009). In both cases, CO_2 is retained either in form of carbonate minerals (mineral trapping) or dissolved in solution (solubility trapping) (e.g., Baines et al., 2004; Bradshaw et al., 2005) leading to decreased $CO_2/^3He$ ratios and more negative $\delta^{13}C$ in the residual gases.

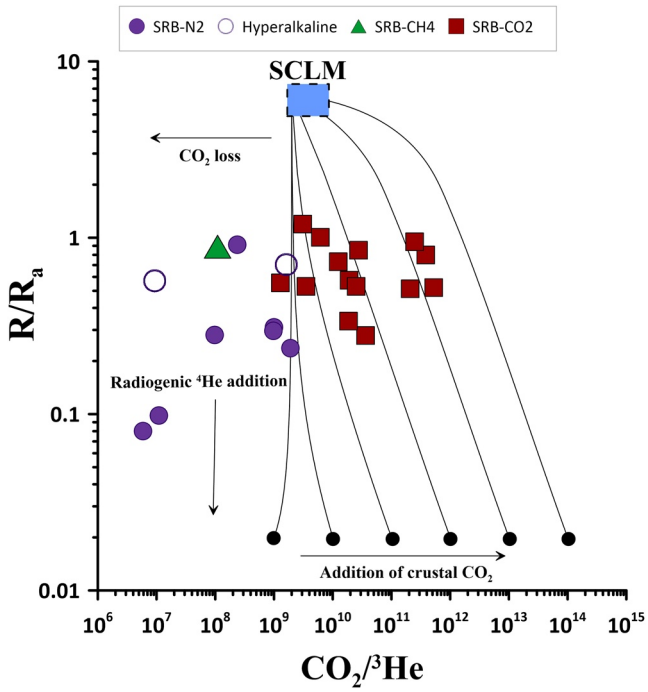

Figure 6. $^{3}He/^{4}He$ (expressed as R/Ra) versus $CO_2/^{3}He$ ratio plot of the sampled gases. Binary mixing curves are shown between the SCLM (6.1 ± 0.9 Ra and $CO_2/^{3}He$ of 7×10^{9}; Bräuer et al., 2016; Gautheron & Moreira, 2002) and different hypothetical crustal end-members with same helium isotopic composition (0.02 Ra) but variable $CO_2/^{3}He$ ratios. N_2-dominated, CH_4-dominated, and alkaline springs require CO_2 loss via gas-water-rock interactions.

In order to interpret the variability of $CO_2/^{3}He$ ratios coupled to that of $\delta^{13}C$ that we recognized in the Vardar zone samples, we investigate the processes of CO_2 partial dissolution in water, and calcite precipitation, by modeling (see Gillfillan et al., 2009) their potential control on $CO_2/^{3}He$ ratios and CO_2 carbon isotopic compositions ($\delta^{13}C$) (Figure 7). According to Gillfilan et al. (2009), the process can be modeled as (a) an open-system degassing (Rayleigh type) at isotopic equilibrium (between phases) and (b) calcite precipitation (Figure 7). We model the progressive variation of the $CO_2/^{3}He$ ratio in the residual gas assuming that the $CO_2/^{3}He$ ratio and the $\delta^{13}C_{CO2}$ of the pristine gas are of mantle-type ($CO_2/^{3}He$ range = $2–7 \times 10^{-9}$, $\delta^{13}C = -3.5‰$; Bräuer et al., 2016; Marty et al., 2020; Rizzo et al., 2018). We stress that here we consider the case of a pristine gas as the mantle end-member, but the choice of a different end-member, resulting from the mixing between crustal (limestone + organic-biogenic) and mantle-derived fluids, would lead to similar (but shifted) model curves.

Our model curves, obtained over a range of pH values for increasing extents of gas dissolution, are plotted in Figure 7. Overall, we find the model CO_2 dissolution lines at pH between 5.6 and 7 fit the data set nicely. This comparison demonstrates the N_2-dominated samples can be interpreted as due to different degrees of CO_2 loss by dissolution, from about 50% (for samples SRB 14, SRB 25, SRB 26) to about 99% for more fractionated samples. These gas/water fractionations ultimately result in ^{13}C-depleted compositions and $CO_2/^{3}He$ spanning over 3 orders of magnitude.

We caution that, for a thick crustal sector with a potentially high number of stratified aquifer such as in Serbia, a simple open-system degassing (Rayleigh type) model approach is evidently a simplified approach. In fact, it is possible that more complex gas-aquifer interactions, such as complete gas dissolution in deep aquifer, followed by multistep degassing upon groundwater upward migration (Chiodini et al., 2011), could have taken place instead. Also, we cannot exclude the lowest $\delta^{13}C_{CO2}$ values are not at least partially reflecting a biogenic origin, and carbonate precipitation (together with CO_2 dissolution at a lower pH than 5.6–7; Gillfillan et al., 2009) has not taken a role. This notwithstanding, although simplified, our model clearly highlights the role played by gas-water interaction in determining the composition of Serbian gas manifestations.

5.2. Mantle Helium Source and Tectonic Implications

The chemistry of both CO_2-dominated and N_2-dominated gas samples unravels the active outgassing of mantle-derived volatiles (He and, to a lesser extent, CO_2) in Serbia. In continental areas far from any evidence of active volcanism, the possible main sources of mantle-derived volatiles are (a) reservoirs of fossil mantle-derived volatiles (e.g., Ballentine et al., 2001), (b) the presence of magmatic intrusions into the crust, and (c) the transfer of mantle He through lithospheric faults (e.g., Burnard et al., 2013; Caracausi & Sulli, 2019; Kennedy et al., 2007; Lee et al., 2019). A reservoir of fossil mantle-derived volatiles as a source of the mantle He should not be associated to a heat-excess, as presently observed at regional scale in Serbia (up to 130 mW/m^2). Magmatic intrusions in the crust could in principle supply both mantle-derived heat and fluids toward the surface. However, at a regional scale, a magmatic intrusion can be considered as a localized source of both volatiles and heat. In spite of some possible long-range transport through groundwaters, the He isotopic ratio and heat flux anomaly should thus decrease upon increasing distance from the position of the source at depth. In the study area, in contrast, we recognize a fairly homogeneous and generalized outgassing of mantle-derived He (Figure 1) and high regional heat flow. Therefore, it is unlikely that isolated magmatic intrusions in the crust are involved.

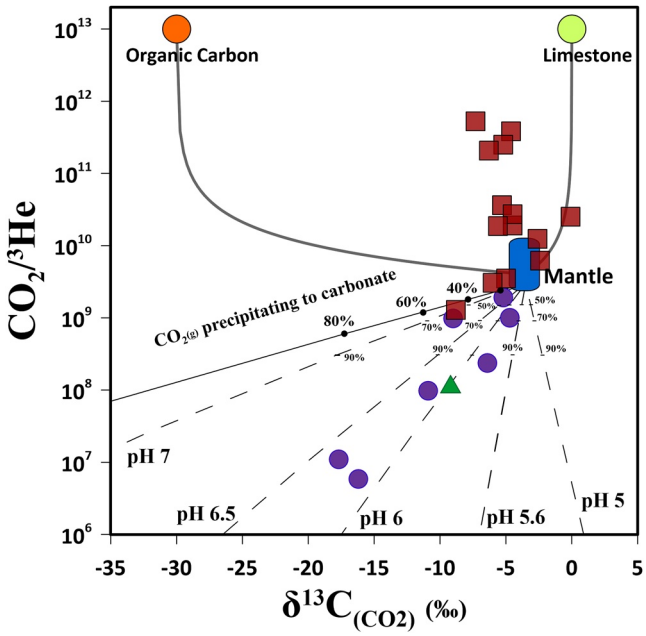

Figure 7. Plot of $\delta^{13}C_{(CO2)}$ versus $CO_2/^3He$. The predicted model lines for Rayleigh-type gas dissolution at different pHs are shown as broken lines, while the solid lines are the predicted trend for carbonate mineral precipitation. Changes in $\delta^{13}C_{(CO2)}$ are calculated following the method from Gillfillan et al. (2009) using the Rayleigh fractionation equation either for precipitation or for dissolution. In the case of precipitation there is zero ^3He loss from the CO_2 phase and $CO_2/^3He$ changes in proportion to the fraction of the remaining CO_2 phase while for CO_2 dissolution, the change in $CO_2/^3He$ ratio is calculated following the Rayleigh equation.

Volatiles (i.e., CO_2, He) can reach the surface directly from the mantle through lithospheric faults (e.g., Burnard et al., 2012; Caracausi & Sulli, 2019; Lee et al., 2019), acting as a network of pathways of high permeability enhancing the transfer of deep fluids and heat through the crust. The study area is strongly affected by active tectonics as indicated by seismicity (http://www.seismo.gov.rs/Seizmicnost/Katalog-zemljotresa.pdf.). All the investigated emissions are located along tectonic discontinuities, even if all of them are not in correspondence of the main regional faults (Figure 1). Hence, a system of well-connected faults with roots down to the mantle, through which the fluids and heat from the mantle can cross the crust and reach the surface, seems the most plausible mechanism to explain the combined high heat flux and regional-scale outgassing of mantle He in the study area.

In Serbia, crustal thickness progressively increases in ~260 km, from about 25 km in the north up to 35 km in the south (Horváth et al., 2015; Marovic et al., 2007). The greater thickness in the south of Serbia could lead to a higher production of ^4He by the U and Th decay if we assume a homogeneous and constant distribution of U and Th concentrations in the crust below the study area. However, we find no geographical control on He isotopic signature, and a large He isotope variability occurs sometimes over short distances (e.g., 1 order of magnitude change in only 27 km) (see Figure S1 in Supporting Information S1). Therefore, the variability of the He isotopic signature does not appear to correlate with crustal thickness. Moreover, we highlight that the lowest He isotopic signatures (SRB10 site, 0.08 Ra; SRB11 site, 0.10 Ra) have been measured in fluids that circulate in U-rich and Th-rich granitic rocks. Thus, it is reasonable that the lowest He isotopic signatures could be due to local high production of ^4He (Figure S1 in Supporting Information S1; Section b) from granitoid lithologies.

A quantitative He flux estimate can provide insights into the transfer of volatiles through the crust. Estimates of the ^4He flux in continental regions are mainly based on calculations of in-situ production and steady-state degassing through the continental crust, and these calculations yield a crustal ^4He degassing flux of $\sim 3.3 \pm 0.5 \times 10^{10}$ atoms m^{-2} s^{-1} (Buttitta et al., 2020, and references therein). However, experimental work highlights that the release of volatiles from rock increases in an active stress field, which implies that ^4He degassing through the crust can be episodic in active tectonic areas (e.g., Bräuer et al., 2016; Honda et al., 1982; Torgersen & O'Donnell, 1991). It is worthy of note that deformation and failure of rocks crack mineral grains, causing pervasive microfracturing. Consequently, the rocks can increase their porosities from 20% to as high as 400% prior to failure, opening new microfracture surfaces, and eventually causing macroscopic failure and fracture of rocks (Bräuer et al., 2016). These processes lead to a higher release of volatiles (e.g., He) previously trapped within mineral grains along fracture networks and the pore fluids transport these volatiles through the crust.

Considering that, during the transfer of mantle-derived fluids through the crust, the addition of crustal radiogenic ^4He produces a decrease of the pristine mantle He isotopic ratio, it is possible to assess the flux of mantle-derived He by using the approach proposed by O'Nions and Oxburgh (1988) and making a guess for the crustal He flux range. This method is based on the assumption that, if the degassing of He occurs at steady state, then it is possible to estimate the mantle He flux from the helium isotope composition of the system. This principle is illustrated in Figure 8 that shows the dependence of R/Ra in the surface gas on mantle He flux (for a crustal ^4He flux of $3.3 \pm 0.5 \times 10^{10}$ atoms m^{-2} s^{-1}). From this, we estimate a mantle-derived He flux in the study area of $\sim 2.1 \times 10^8$ to $\sim 9.0 \times 10^9$ atoms m^{-2} s^{-1}, up to 2 orders of magnitude higher than normally found in stable continental areas ($<<10^8$; e.g., O'Nions & Oxburgh, 1988).

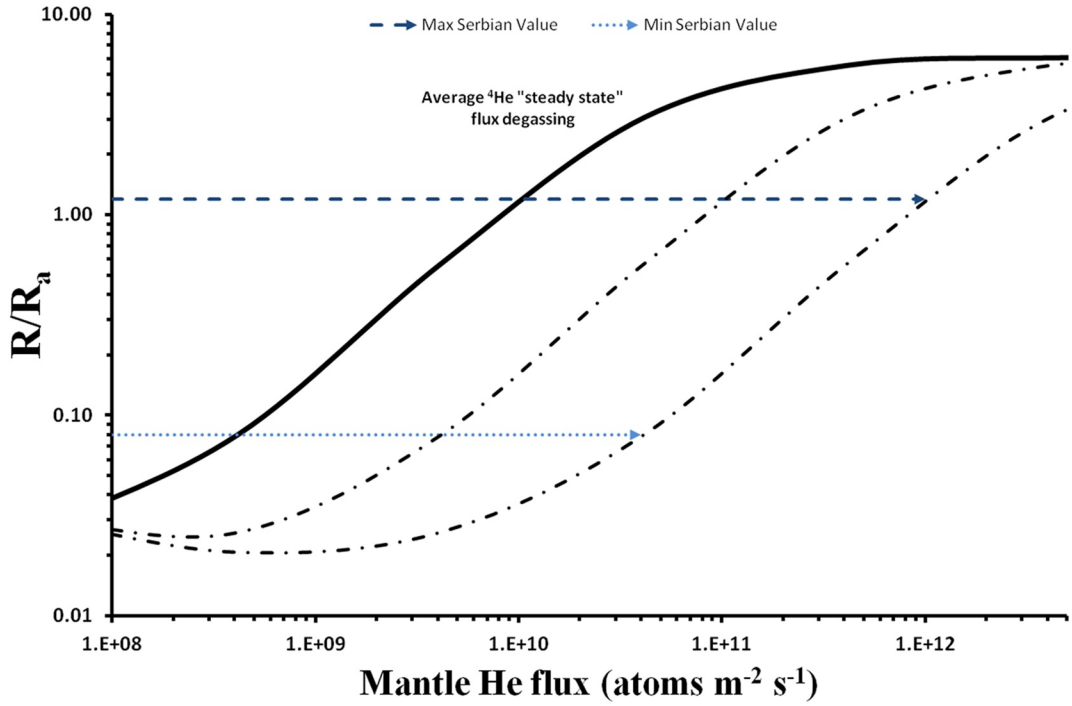

Figure 8. Helium isotope composition versus the flux of mantle-derived He. The lines are computed by using the approach proposed by O'Nions and Oxburgh (1988) that is based on the progressive addition (as a mixing) of a crustal He component that dilute the mantle He component producing a decrease of the He isotopic signature from the typical mantle-derived component (6.1 Ra; Gautheron & Moreira, 2002) to the radiogenic signature (0.02 Ra; Ballentine & Burnard, 2002). The solid curve refers to an average continental crust ^{4}He steady-state flux of $3.3 \pm 0.5 \times 10^{10}$ atoms m^{-2} s^{-1} (Buttitta et al., 2020). The dotted curves refer to 10× and 100× the average continental crust steady-state He flux. The blue dotted line corresponds to minimum and dark blue dashed line to maximum R/Ra values in our samples, and are used to infer the mantle He flux range in Serbia region.

However, in active tectonic regions an enhanced release of He from rocks occurs that is up to 10^4 times higher the steady-state values. Therefore, assuming a ^{4}He crustal flux of 10–10^4 times the average "steady-state" value, the mantle He fluxes increase to between 10^{11} and 10^{14} atoms m^{-2} s^{-1} (Figure 8). These are typical He fluxes encountered in active tectonic regions and/or in volcanic systems (Figure 9; Torgersen, 2010).

Active fault zones are regions of advanced permeability that permit a fast transfer of volatiles through the crust, and seismicity is a strong evidence of the capacity of faults to transfer fluids through the crust. However, the mechanisms that control the migration of fluids in the deep crust (e.g., ductile layers) are still not well recognized (e.g., Caracausi & Sulli, 2019; Kulongoski et al., 2005). In active tectonic regions, fluids can move via developing fault-fracture meshes with a mechanism analogous to the fault valve model that drives flow by fluid over-pressurization and stress switching (compression to extension) (Newell et al., 2015; Sibson, 2013, 2020), or by creep cavitation that can establish a dynamic granular fluid pump in ductile shear zones (i.e., Fusseis et al., 2009). Therefore, considering: (a) that the study area is affected by extensional tectonics and active seismicity down to the crust-mantle boundary (Faccenna et al., 2014; Marović et al., 2007; Metois et al., 2015); (b) the high regional heat flow (up to 130 mW/m^2) due to the up-rise of the asthenosphere up to 50–60-km depth at regional scale (Horváth et al., 2015), (c) the presence of inherited lithospheric tectonic discontinues that allowed the up-rise of magmas since the Jurassic (Zelić et al., 2010), and that can still work today as pathways for the transfer of deep volatiles through the crust, (d) the computed high fluxes of mantled derived He, we conclude that the mantle below Serbia is the most obvious source of the surface-released heat and fluids.

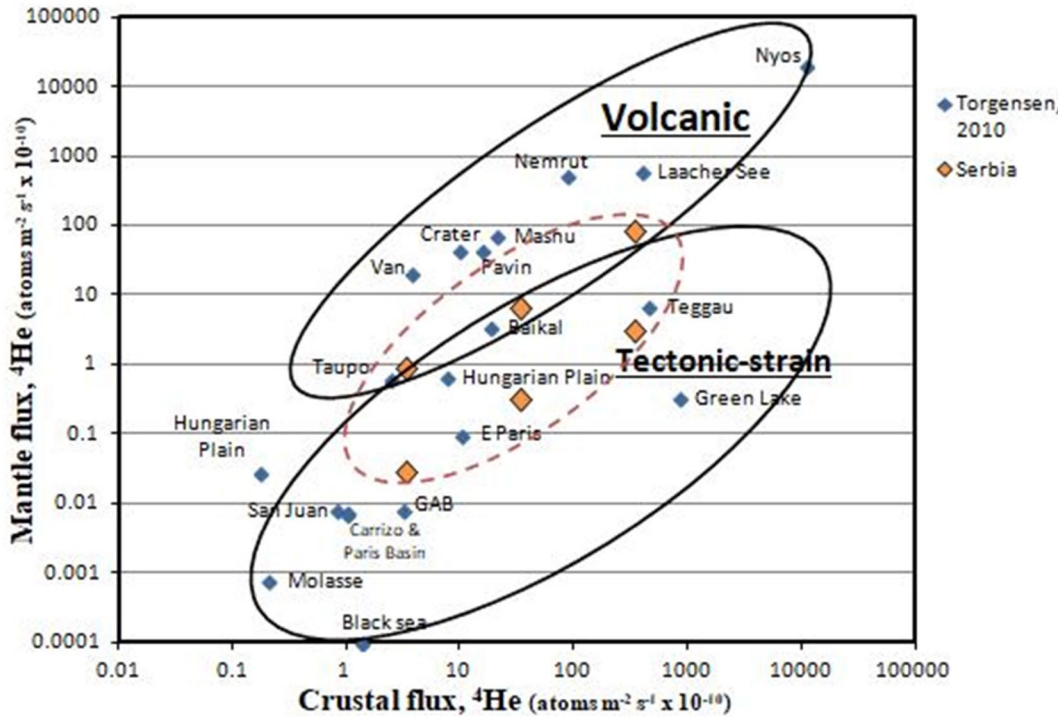

Figure 9. Crustal-derived He fluxes in Serbia compared with mantle-derived He fluxes estimated by using the approach proposed by O'Nions and Oxburgh (1988). The assessed mantle-derived He flux for the Serbian gases (orange diamonds), using the highest R/Ra value, is ~9.0×10^9 atoms m^{-2} s^{-1} while for the lowest R/Ra value the mantle-derived He flux is ~3×10^9 atoms m^{-2} s^{-1}. For crustal-derived ^{4}He fluxes being 10–10^4 times higher than the "steady-state" crust, the mantle helium fluxes would also be in the order of magnitude of values characteristic of "Volcanic field" and/or "Tectonic-strain field" (red dotted ellipse area; modified after Torgensen [2010]). The six orange diamonds (Serbian point) represent, respectively, the mantle ^{4}He flux values for maximum and minimum R/Ra calculated on the base of continental crust ^{4}He production ($3.3 \pm 0.5 \times 10^{10}$ atoms m^{-2} s^{-1}; Buttitta et al., 2020) and for 10 times and 100 times this value.

6. Conclusions

We investigated the chemical and isotopic composition of natural gas manifestations along the Serbian Vardar zone, a mega-suture zone between the Eurasia and the African plate. Gas compositions are very heterogeneous and cluster into the groups of CO_2-dominated, N_2-dominated, and CH_4-dominated gases. Based on their He isotope compositions (<1.19 Ra), the CO_2-rich samples are interpreted as mixtures of crustal CO_2-rich gas (from limestones and organic matter) and mantle-derived components. The latter accounts for up to 20% of He (Figure 10). N_2-dominated samples are more atmospheric/crustal in nature (mantle He, <5%), and are inferred to have experienced extensive chemical and isotopic fractionations during water-gas-rock interactions in shallow crustal layers (Figure 10).

We estimate a mantle-derived He flux of ~2.1×10^8 to ~9.0×10^9 atoms m^{-2} s^{-1}, or 2 orders of magnitude higher than normally found in stable continental areas. This elevated transport of mantle-derived volatiles in the Serbian crustal sector is interpreted to occur through lithospheric faults that work as regions of enhanced permeability and favor the migration of fluids thought the whole crust (Figure 10). Our study thus confirms that elevated outgassing of mantle-derived fluids can occur in tectonically active continental regions, even far from active volcanism (e.g., Caracausi & Sulli, 2019; Chiodini et al., 2004; Lee et al., 2019; Tamburello et al., 2018). Finally, we recognize that at regional scale the mantle volatiles are sourced directly from the mantle together with heat and this scenario supports the asthenosphere up-rise and delamination processes at the mantle-crust boundary recognized by recent regional geophysical investigations (Belinić et al., 2021).

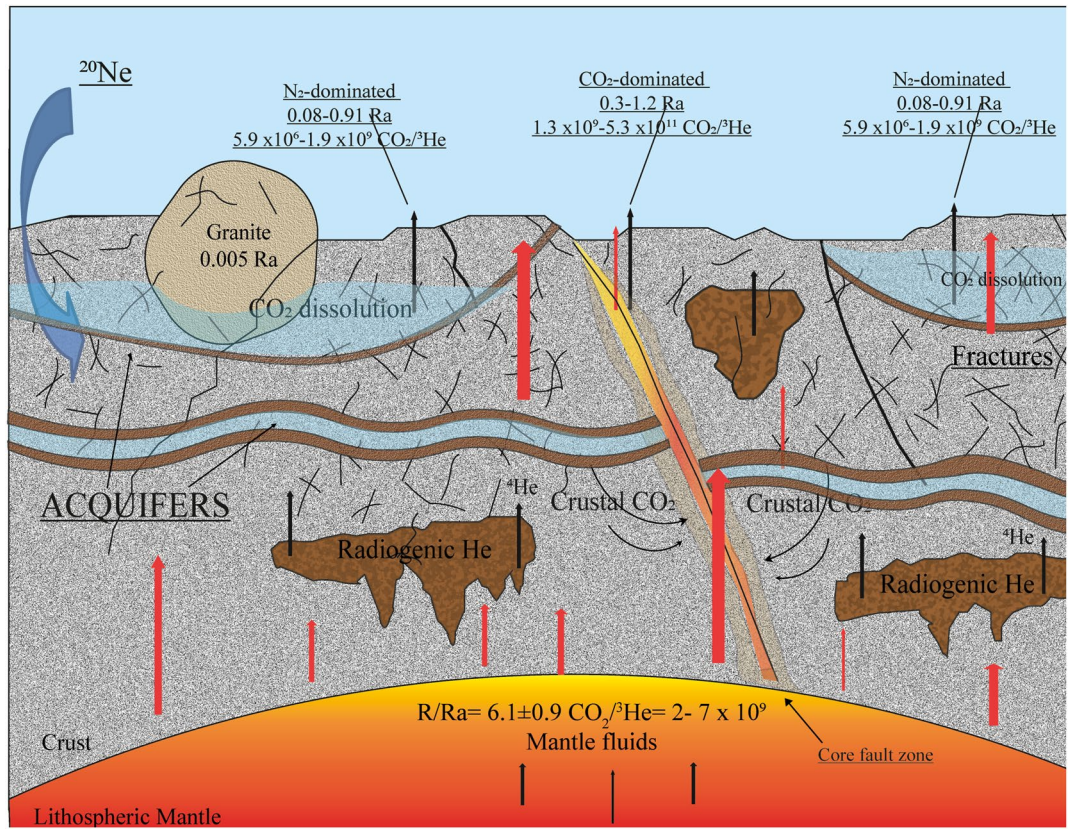

Figure 10. Cross section cartoon showing the scenario proposed for the possible source, volatile pathways, and secondary processes (dissolution, radiogenic addition). Not to scale. Brown bodies are fossil intrusions which could be present deep under the surface. Red arrows indicate the heat flux.

Data Availability Statement

Randazzo et al. (2021, http://doi.org/10.26022/IEDA/112164).

Acknowledgments
This work was supported by MIUR project PRIN2017-2017LMNLAW "Connect4Carbon" and DCO Grant 10881-TDB "Improving the estimation of tectonic carbon flux", by the European Union and the State of Hungary, co-financed by the European Regional Development Fund in the project of GINOP-2.3.2-15-2016-00009 "ICER" and by UBB grant nr GTC 35290/18.11.2020. Field work was supported by Brem Group Belgrade. The authors thank INGV-Palermo for supporting the analysis carried out in its laboratories and Mariano Tantillo, Aldo Sollami, Ygor Oliveri, and Francesco Salerno (gases chemistry, noble-gas, and stable isotopes) for their analytical contribution. The authors also thank the two anonymous reviewers for their critical comment which contributed to improve the manuscript.

References

Aeschbach-Hertig, W., Kipfer, R., Hofer, M., Imboden, D. M., Wieler, R., & Signer, P. (1996). Quantification of gas fluxes from the subcontinental mantle: The example of Laacher See, a Maar lake in Germany. *Geochimica et Cosmochimica Acta*, *60*, 31–41. https://doi.org/10.1016/0016-7037(95)00370-3

Baciu, C., Caracausi, A., Etiope, G., & Italiano, F. (2007). Mud volcanoes and methane seeps in Romania: Main features and gas flux. *Annals of Geophysics*, *50*(4), 501–511.

Baines Shelagh, J., & Worden Richard, H. (2004). The long-term fate of CO_2 in the subsurface: Natural analogues for CO_2 storage. *Geological Society, London, Special Publications*, *233*(1), 59–85. https://doi.org/10.1144/GSL.SP.2004.233.01.06

Ballentine, C. J., Burgess, R., & Marty, B. (2002). Tracing fluid origin, transport and interaction in the crust. In D. R. Porcelli, C. J. Ballentine, & R. Weiler (Eds.), *Noble gases in geochemistry and cosmochemistry* (pp. 539–614). Geochemical Society and Mineralogical Society of America. https://doi.org/10.1515/9781501509056-015

Ballentine, C. J., & Burnard, P. (2002). Production, release and transport of noble gases in the continental crust. *Reviews in Mineralogy and Geochemistry*, *47*(1), 481–538. https://doi.org/10.2138/rmg.2002.47.12

Ballentine, C. J., O'Nions, R. K., Oxburgh, E. R., Horvath, E., & Deak, J. (1991). Rare gas constraints on hydrocarbon accumulation, crustal degassing and groundwater flow in the Pannonian Basin. *Earth and Planetary Science Letters*, *105*, 229–246. https://doi.org/10.1016/0012-821X(91)90133-3

Ballentine, C. J., Schoell, M., Coleman, D., & Cain, B. A. (2001). 300-Myr-old magmatic CO_2 in natural gas reservoir of the west Texas Permian basin. *Nature*, *409*(6818), 327–331. https://doi.org/10.1038/35053046

Ballentine, C. J., & Sherwood Lollar, B. (2002). Regional groundwater focusing of nitrogen and noble gases into the Hugoton-Panhandle giant gas field, USA. *Geochimica et Cosmochimica Acta*, *66*, 2483–2497. https://doi.org/10.1016/S0016-7037(02)00850-5

Barry, P. H., Negrete-Aranda, R., Spelz, R. M., Seltzer, A. M., Bekaert, D. V., Virrueta, C., & Kulongoski, J. T. (2020). Volatile sources, sinks and pathways: A helium-carbon isotope study of Baja California fluids and gases. *Chemical Geology*, *550*(2020), 119722. https://doi.org/10.1016/j.chemgeo.2020.119722

Bazylev, B., Popević, A., Karamata, S., Kononkova, N. N., Simakin, S. G., Olujić, J., et al. (2009). Mantle peridotites from the Dinaridic ophiolite belt and the Vardar zone western belt, central Balkan: A petrological comparison. *Lithos*, *108*, 37–71. https://doi.org/10.1016/j.lithos.2008.09.011

Belinić, T., Kolínský, P., & Stipčević, J. (2021). Shear-wave velocity structure beneath the Dinarides from the inversion of Rayleigh-wave dispersion. *Earth and Planetary Science Letters*, *555*, 116686. https://doi.org/10.1016/j.epsl.2020.116686

Bortolotti, V., Chiari, M., Marcucci, M., Photiades, P., Principi, G. & Saccani, E. (2008). New geochemical and age data on the ophiolites from the Othrys area (Greece): Implication for the Triassic evolution of the Vardar Ocean. *Ofioliti*, *33*, 135–151.

Bradshaw, J., Boreham, C., & La Pedalina, F. (2005). Storage retention time of CO_2 in sedimentary basins: Examples from petroleum systems. In E. Rubin, D. Keith, & C. Gilboy (Eds.), *Proceedings of the 7th International Conference on Greenhouse Gas Control Technologies* (pp. 541–549). Elsevier Science. https://doi.org/10.1016/b978-008044704-9/50055-0

Bräuer, K., Geissler, W. H., Kämpf, H., Niedermann, S., & Rman, N. (2016). Helium and carbon isotope signatures of gas exhalations in the westernmost part of the Pannonian Basin (SE Austria/NE Slovenia): Evidence for active lithospheric mantle degassing. *Chemical Geology*, *422*, 60–70. https://doi.org/10.1016/j.chemgeo.2015.12.016

Bräuer, K., Kämpf, H., Niedermann, S., & Strauch, G. (2005). Evidence for ascending upper mantle-derived melt beneath the Cheb basin, central Europe. *Geophysical Research Letters*, *32*, L08303. https://doi.org/10.1029/2004GL022205

Bräuer, K., Kämpf, H., Niedermann, S., & Strauch, G. (2013). Indications for the existence of different magmatic reservoirs beneath the Eifel area (Germany): A multi-isotope (C, N, He, Ne, Ar) approach. *Chemical Geology*, *356*, 193–208. https://doi.org/10.1016/j.chemgeo.2013.08.013

Bräuer, K., Kämpf, H., Niedermann, S., Strauch, G., & Tesar, J. (2008). Natural laboratory NW Bohemia: Comprehensive fluid studies between 1992 and 2005 used to trace geodynamic processes. *Geochemistry, Geophysics, Geosystems*, *9*, Q04018. https://doi.org/10.1029/2007GC001921

Bräuer, K., Kämpf, H., Niedermann, S., Strauch, G., & Weise, S. M. (2004). Evidence for a nitrogen flux directly derived from the European Subcontinental Mantle in the western Eger Rift, central Europe. *Geochimica et Cosmochimica Acta*, *68*, 4935–4947. https://doi.org/10.1016/j.gca.2004.05.032

Broadley, M. W., Bekaert, D. V., Marty, B., Yamaguchi, A., & Barrat, J. A. (2020). Noble gas variations in ureilites and their implications for ureilite parent body formation. *Geochimica et Cosmochimica Acta*, *270*, 325–337. https://doi.org/10.1016/j.gca.2019.11.032

Burić, M., Nikić, Z., & Papić, P. (2016). Mineral waters of Montenegro. In P. Papic (Ed.), *Mineral and thermal waters of southeastern Europe. Environmental Earth Sciences* (pp. 65–79). Springer. https://doi.org/10.1007/978-3-319-25379-4_4

Burnard, P., Bourlange, S., Blard, P. H., Geli, L., Tryon, M. D., Natal'in, B., et al. (2012). Constraints on fluid origins and migration velocities along the Marmara main fault (Sea of Marmara, Turkey) using helium isotopes. *Earth and Planetary Science Letters*, *341–344*, 68–78. https://doi.org/10.1016/j.epsl.2012.05.042

Burnard, P., Zimmermann, L., & Sano, Y. (2013). The noble gases as geochemical tracers: History and background. In P. Burnard (Ed.), *The noble gases as geochemical tracers. Advances in isotope geochemistry* (pp. 1–15). Springer. https://doi.org/10.1007/978-3-642-28836-4_1

Buttitta, D., Caracausi, A., Chiaraluce, L., Favara, R., Gasparo Morticelli, M., & Sulli, A. (2020). Continental degassing of helium in an active tectonic setting (northern Italy): The role of seismicity. *Nature Scientific Reports*, *10*, 162. https://doi.org/10.1038/s41598-019-55678-7

Caracausi, A., Martelli, M., Nuccio, M., Paternoster, M., & Stuart, F. M. (2013). Active degassing of mantle-derived fluids; a geochemical study along the Vulture Line, Southern Appennines. *Journal of Volcanology and Geothermal Research*, *253*, 65–74. https://doi.org/10.1016/j.jvolgeores.2012.12.005

Caracausi, A., & Sulli, A. (2019). Outgassing of mantle volatiles in compressional tectonic regime away from volcanism: The role of continental delamination. *Geochemistry, Geophysics, Geosystems*, *20*, 2007–2020. https://doi.org/10.1029/2018GC008046

Carreira, P. M., Marques, J. M., Carvalho, M. R., Capasso, G., & Grassa, F. (2009). Mantle-derived carbon in Hercynian granites. Stable isotopes signatures and C/He associations in the thermomineral waters, N-Portugal. *Journal of Volcanology and Geothermal Research*, *189*(1–2), 49–56. https://doi.org/10.1016/j.jvolgeores.2009.10.008

Chiodini, G., Caliro, S., Cardellini, C., Frondini, F., Inguaggiato, S., & Matteucci, F. (2011). Geochemical evidence for and characterization of CO_2 rich gas sources in the epicentral area of the Abruzzo 2009 earthquakes. *Earth and Planetary Science Letters*, *304*(3–4), 389–398. https://doi.org/10.1016/j.epsl.2011.02.016

Chiodini, G., Cardellini, C., Amato, A., Boschi, E., Caliro, S., Frondini, F., & Ventura, G. (2004). Carbon dioxide degassing and seismogenesis in central southern Italy. *Geophysical Research Letter*, *31*, L07615. https://doi.org/10.1029/2004GL019480

Chiodini, G., Cardellini, C., Di Luccio, F., Selva, J., Frondini, F., Caliro, S., et al. (2020). Correlation between tectonic CO_2 Earth degassing and seismicity is revealed by a 10-year record in the Apennines, Italy. *Science Advances*, *6*(35), eabc2938. https://doi.org/10.1126/sciadv.abc2938

Clever, H. L. (1979). Helium and neon-International Union of Pure and Applied Chemistry. *IUPAC Solubility Data Series* (Vol. *1*).

Cvetković, V., Prelević, D., Downes, H., Jovanović, M., Vaselli, O., & Pecskay, Z. (2004). Origin and geodynamic significance of Tertiary post-collisional basaltic magmatism in Serbia (central Balkan Peninsula). *Lithos*, *73*(3–4), 161–186. https://doi.org/10.1016/j.lithos.2003.12.004

Cvetković, V., Prelević, D., & Pécskay, Z. (2000). Lamprophyric rocks of the Miocene Borac eruptive complex (Central Serbia, Yugoslavia). *Acta Geologica Hungarica*, *43*(1), 25–41.

Cvetković, V., Prelević, D., & Schmid, S. (2016). Geology of south-eastern Europe. In P. Papic (Ed.), *Mineral and thermal waters of southeastern Europe* (pp. 1–29). Springer International Publishing. https://doi.org/10.1007/978-3-319-25379-4_1

D'Alessandro, W., Li Vigni, L., Gagliano, A. L., Calabrese, S., Kyriakopoulos, K., & Daskalopoulou, K. (2020). CO_2 release to the atmosphere from thermal springs of Sperchios Basin and northern Euboea (Greece): The contribution of "hidden" degassing. *Applied Geochemistry*, *119*, 104660. https://doi.org/10.1016/j.apgeochem.2020.104660

Daskalopoulou, K., Gagliano, A. L., Calabrese, S., & D'Alessandro, W. (2019). Estimation of the geogenic carbon degassing of Greece. *Applied Geochemistry*, *106*, 60–74. https://doi.org/10.1016/j.apgeochem.2019.04.018

De Leeuw, G. A. M., Hilton, D. R., Güleç, N., & Mutlu, H. (2010). Regional and temporal variations in $CO_2/^3He$, $^3He/^4He$ and $\delta^{13}C$ along the North Anatolian Fault Zone, Turkey. *Applied Geochemistry*, *25*, 524–539. https://doi.org/10.1016/j.apgeochem.2010.01.010

Djordjević, M. (2005). Volcanogenic Turonian and epiclastics of Senonian in the Timok Magmatic Complex between Bor and the Tupižnica Mountain (eastern Serbia). *Annales Géologiques de la Péninsula Balkanique*, *66*, 63–71. https://doi.org/10.2298/gabp0566063d

Dogan, T., Sumino, H., Nagao, K., Notsu, K., Tuncer, M. K., & Celik, C. (2009). Adjacent releases of mantle helium and soil CO_2 from active faults: Observations from the Marmara region of the North Anatolian Fault zone, Turkey. *Geochemistry, Geophysics, Geosystems*, *10*, Q11009. https://doi.org/10.1029/2009GC002745

Doljak, D., & Jojić Glavonjić, T. (2016). State and prospects of geothermal energy usage in Serbia. *Journal of Geographical Institute "Jovan Cvijic"*, *66*(2), 221–236. https://doi.org/10.2298/IJGI1602221D

Etiope, G., Caracausi, A., Favara, R., Italiano, F., & Baciu, C. (2003). Reply to comment by A. Kopf on "Methane emission from the mud volcanoes of Sicily (Italy)", and notice on CH_4 flux data from European mud volcanoes. *Geophysical Research Letters*, *30*, 1094. https://doi.org/10.1029/2002GL016287

Etiope, G., Caracausi, A., Italiano, F., Baciu, C., & Cosma, C. (2004). Gas flux to the atmosphere from mud volcanoes in eastern Romania. *Terra Nova*, *16*, 179–184. https://doi.org/10.1111/j.1365-3121.2004.00542.x

Faccenna, C., Becker, T. W., Auer, L., Billi, A., Boschi, L., Brun, J. P., et al. (2014). Mantle dynamics in the Mediterranean. *Reviews of Geophysics*, *52*, 283–332. https://doi.org/10.1002/2013RG000444

Frunzeti, N. (2013). *Geogenic emissions of greenhouse gases in the Southern part of the Eastern Carpathians* (doctoral dissertation). Babes-Bolyai University, Faculty of Environmental Science and Engineering. (in Romanian).

Fusseis, F., Regenauer-Lieb, K., Liu, J., Hough, R. M., & De Carlo, F. (2009). Creep cavitation can establish a dynamic granular fluid pump in ductile shear zones. *Nature*, *459*, 974–977. https://doi.org/10.1038/nature08051

Gautheron, C., & Moreira, M. (2002). Helium signature of the subcontinental lithospheric mantle. *Earth and Planetary Science Letters*, *199*(1–2), 39–47. https://doi.org/10.1016/S0012-821X(02)00563-0

Gilfillan, S. M. V., Ballentine, C. J., Holland, G., Blagburn, D., Sherwood Lollar, B., Stevens, S., et al. (2008). The noble gas geochemistry of natural CO_2 gas reservoirs from the Colorado Plateau and Rocky Mountain provinces, USA. *Geochimica et Cosmochimica Acta*, *72*, 1174–1198. https://doi.org/10.1016/j.gca.2007.10.009

Gilfillan, S. M. V., Lollar, B. S., Holland, G., Blagburn, D., Stevens, S., Schoell, M., et al. (2009). Solubility trapping in formation water as dominant CO_2 sink in natural gas fields. *Nature*, *458*(7238), 614–618. https://doi.org/10.1038/nature07852

Holland, G., & Gilfillan, S. (2013). Application of noble gases to the viability of CO_2 storage. In P. Burnard (Ed.), *The noble gases as geochemical tracers. Advances in isotope geochemistry* (pp. 177–223). Springer. https://doi.org/10.1007/978-3-642-28836-4_8

Honda, M., Kurita, K., Hamano, Y., & Ozima, M. (1982). Experimental studies of He and Ar degassing during rock fracturing. *Earth and Planetary Science Letters*, *59*(2), 429–436. https://doi.org/10.1016/0012-821X(82)90144-3

Horváth, F., Musitz, B., Balázs, A., Végh, A., Uhrin, A., Nádor, A., et al. (2015). Evolution of the Pannonian basin and its geothermal resources. *Geothermics*, *53*, 328–352. https://doi.org/10.1016/j.geothermics.2014.07.009

Ionescu, A., Baciu, C., Kis, B.-M., & Sauer, P. E. (2017). Evaluation of dissolved light hydrocarbons in different geological settings in Romania. *Chemical Geology*, *469*, 230–245. https://doi.org/10.1016/j.chemgeo.2017.04.017

Italiano, F., Kis, B. M., Baciu, C., Ionescu, A., Harangi, S., & Palcsu, L. (2017). Geochemistry of dissolved gases from the eastern Carpathians-Transylvanian Basin boundary. *Chemical Geology*, *469*, 117–128. https://doi.org/10.1016/j.chemgeo.2016.12.019

Italiano, F., Sasmaz, A., Yuce, G., & Okan, O. (2013). Thermal fluids along the East Anatolian Fault Zone (EAFZ): Geochemical features and relationships with the tectonic setting. *Chemical Geology*, *339*, 103–114. https://doi.org/10.1016/j.chemgeo.2012.07.027

Jelenković, R., Kostić, A., Životić, D., & Ercegovac, M. (2008). Mineral resources of Serbia. *Geologica Carpatica*, *59*(4), 345–361.

Kennedy, B. M., & Van Soest, M. C. (2007). Flow of mantle fluids through the ductile lower crust: Helium isotope trends. *Science*, *318*(5855), 1433–1436. https://doi.org/10.1126/science.1147537

Kis, B. M., Caracausi, A., Palcsu, L., Baciu, C., Ionescu, A., Futó, I., et al. (2019). Noble gas and carbon isotope systematics at the seemingly inactive Ciomadul volcano (Eastern-Central Europe, Romania): Evidence for volcanic degassing. *Geochemistry, Geophysics, Geosystems*, *20*, 3019–3043. https://doi.org/10.1029/2018GC008153

Kis, B. M., Ionescu, A., Cardellini, C., Harangi, S., Baciu, C., Caracausi, C., & Viveiros, F. (2017). Quantification of carbon dioxide emissions of Ciomadul, the youngest volcano of the Carpathian-Pannonian Region (Eastern-Central Europe, Romania). *Journal of Volcanology and Geothermal Research*, *341*, 119–130. https://doi.org/10.1016/j.jvolgeores.2017.05.025

Kulongoski, J. T., Hilton, D. R., & Izbicki, J. A. (2005). Source and movement of helium in the eastern Morongo groundwater basin: The influence of regional tectonics on crustal and mantle helium fluxes. *Geochimica et Cosmochimica Acta*, *69*, 3857–3872. https://doi.org/10.1016/j.gca.2005.03.001

Labidi, J., Barry, P. H., Bekaert, D. V., Broadley, M. W., Marty, B., Giunta, T., et al. (2020). Hydrothermal $^{15}N^{15}N$ abundances constrain the origins of mantle nitrogen. *Nature*, *580*, 367–371. https://doi.org/10.1038/s41586-020-2173-4

Lee, H., Kim, H., Kagoshima, T., Park, J., Takahata, N., & Sano, Y. (2019). Mantle degassing along strike-slip faults in the Southeastern Korean Peninsula. *Nature Scientific Report*, *9*, 15334. https://doi.org/10.1038/s41598-019-51719-3

Lenkey, L., Dövényi, P., Horváth, F., & Cloetingh, S. A. P. L. (2002). *Geothermics of the Pan-Nonian Basin and its bearing on the neotectonics* (Vol. *3*, pp. 1–12). EGU Stephan Mueller Special Publication Series. https://doi.org/10.5194/smsps-3-29-2002

Lowenstern, J. B., Evans, W. C., Bergfeld, D., & Hunt, A. G. (2014). Prodigious degassing of a billion years of accumulated radiogenic helium at Yellowstone. *Nature*, *506*, 355–358. https://doi.org/10.1038/nature12992

Mamyrin, B. A., & Tolstikhin, I. N. (1984). Helium isotopes in nature. In *Developments in geochemistry*. Elsevier Science Ltd.

Marović, M., Djoković, I., Pešić, L., Radovanović, S., Toljić, M., & Gerzina, N. (2002). Neotectonics and seismicity of the southern margin of the Pannonian Basin in Serbia. *EGU Stephan Mueller Special Publication Series*, *3*, 277–295.

Marović, M., Toljić, M., Rundić, L., & Milivojević, J. (2007). *Neoalpine tectonics of Serbia* (p. 87 and map). Serbian Geological Society, Ser. Monographie.

Marty, B., Almayrac, M., Barry, P. H., Bekaert, D. V., Broadley, M. W., Byrne, D. J., et al. (2020). An evaluation of the C/N ratio of the mantle from natural CO_2-rich gas analysis: Geochemical and cosmochemical implications. *Earth and Planetary Science Letters*, *551*(2020), 116574. https://doi.org/10.1016/j.epsl.2020.116574

Métois, M., D'Agostino, N., Avallone, A., Chamot-Rooke, N., Rabaute, A., Duni, L., et al. (2015). Insights on continental collisional processes from GPS data: Dynamics of the peri-Adriatic belts. *Journal of Geophysical Research: Solid Earth*, *120*, 8701–8719. https://doi.org/10.1002/2015JB012023

Milivojević, M. (1993). Geothermal model of Earth's crust and lithosphere for the territory of Yugoslavia: Some tectonic implications. *Studia Geophysica et Geodaetica*, *37*, 265–278. https://doi.org/10.1007/BF01624600

Minissale, A., Magro, G., Martinelli, G., Vaselli, O., & Tassi, F. (2000). Fluid geochemical transect in the Northern Apennines (central-northern Italy): Fluid genesis and migration and tectonic implications. *Tectonophysics*, *319*, 199–222. https://doi.org/10.1016/S0040-1951(00)00031-7

Moores, E. M., & Fairbridge, R. W. (Eds.). (1997). *Encyclopedia of European and Asian regional geology* (p. 804). Chapman and Hall.

Mutlu, H., Güleç, N., & Hilton, D. R. (2008). Helium–carbon relationships in geothermal fluids of western Anatolia, Turkey. *Chemical Geology*, *247*(1–2), 305–321. https://doi.org/10.1016/j.chemgeo.2007.10.021

Newell, D. L., Jessup, M. J., Hilton, D. R., Shaw, C. A., & Hughes, C. A. (2015). Mantle-derived helium in hot springs of the Cordillera Blanca, Peru: Implications for mantle-to-crust fluid transfer in a flat-slab subduction setting. *Chemical Geology*, *417*, 200–209. https://doi.org/10.1016/j.chemgeo.2015.10.003

O'Nions, R. K., & Oxburgh, E. R. (1988). Helium, volatile fluxes and the development of continental crust. *Earth and Planetary Science Letters*, *90*(3), 331–334. https://doi.org/10.1016/0012-821X(88)90134-3

Ozima, M., & Podosek, F. A. (2002). *Noble gas geochemistry* (p. 286). Cambridge University Press.

Palcsu, L., Vetö, I., Futó, I., Vodila, G., Papp, L., & Majo, Z. (2014). In-reservoir mixing of mantle-derived CO_2 and metasedimentary CH_4-N_2 fluids—Noble gas and stable isotope study of two multistacked fields (Pannonian Basin System, W-Hungary). *Marine and Petroleum Geology*, *54*, 216–227. https://doi.org/10.1016/j.marpetgeo.2014.03.013

Pamic, J. (1997). *Volcanic rocks from the Sava-Drava interfluve and Baranja in the South Pannonian Basin (Croatia)* (p. 192). Nafta J. Special Publications, Monograph. (in Croatian with English summary).

Pamić, J., Tomljenović, B., & Balen, D. (2002). Geodynamic and petrogenetic evolution of Alpine ophiolites from the central and NW Dinarides: An overview. *Lithos*, *65*, 113–142. https://doi.org/10.1016/S0024-4937(02)00162-7

Prelevic, D., Foley, S. F., Rome, R. L., Cvetkovic, V., & Downes, H. (2005). Tertiary ultrapotassic volcanism in Serbia: Constraints on petrogenesis and mantle source characteristics. *Journal of Petrology*, *46*, 1443–1487. https://doi.org/10.1093/petrology/egi022

Randazzo, P., Caracausi, A., Aiuppa, A., Cardellini, C., Chiodini, G., D'Alessandro, W., et al. (2021). *Location, chemical and isotopic composition of bubbling gases collected in the central west Serbia, Version 1.0*. Interdisciplinary Earth Data Alliance (IEDA). https://doi.org/10.26022/IEDA/112164

Rizzo, A. L., Pelorosso, B., Coltorti, M., Ntaflos, T., Bonadiman, C., Matusiak-Małek, M., et al. (2018). Geochemistry of noble gases and CO_2 in fluid inclusions from lithospheric mantle beneath Wilcza Góra (Lower Silesia, Southwest Poland). *Frontiers in Earth Science*, *6*, 215. https://doi.org/10.3389/feart.2018.00215

Rosca, M., Bendea, C., & Vîjdea, A. M. (2016). Mineral and thermal waters of Romania. In P. Papic (Ed.), *Mineral and thermal waters of southeastern Europe*. *Environmental Earth Sciences* (pp. 97–114). Springer. https://doi.org/10.1007/978-3-319-25379-4_6

Sano, Y., & Marty, B. (1995). Origin of carbon in fumarolic gas from island arcs. *Chemical Geology*, *119*, 265–274. https://doi.org/10.1016/0009-2541(94)00097-R

Sano, Y., Tominaga, T., & Williams, S. N. (1997). Secular variations of helium and carbon isotopes at Galeras volcano, Colombia. *Journal of Volcanology and Geothermal Research*, *77*(1–4), 255–265. https://doi.org/10.1016/S0377-0273(96)00098-4

Sano, Y., & Wakita, H. (1985). Geographical distribution of $^3He/^4He$ ratios in Japan: Implications for arc tectonics and incipient magmatism. *Journal of Geophysical Research*, *90*(B10), 8729–8741. https://doi.org/10.1029/JB090iB10p08729

Sarbu, S., Aerts, J. W., Flot, J. F., Van Spanning, R. J. M., Baciu, C., Ionescu, A., et al. (2018). Sulfur Cave (Romania), an extreme environment with microbial mats in a CO_2-H_2S/O gas chemocline dominated by mycobacteria. *International Journal of Speleology*, *47*(2), 173–187. https://doi.org/10.5038/1827-806x.47.2.2164

Šarić, K., Cvetković, V., Romer, R. L., Christofides, G., & Koroneos, A. (2009). Granitoids associated with East Vardar ophiolites (Serbia, F.Z.R. of Macedonia and northern Greece): Origin, evolution and geodynamic significance inferred from major and trace element data and Sr–Nd–Pb isotopes. *Lithos*, *108*(1–4), 131–150. https://doi.org/10.1016/j.lithos.2008.06.001

Scharlin, P., & Cargill, R. W. (1996). Carbon dioxide in water and aqueous electrolyte solutions. In *Solubility data series* (Vol. *62*, p. 1996). IUPAC.

Schefer, S., Cvetkovic, V., Fügenschuh, B., Kounov, A., Ovtcharova, M., Schaltegger, U., & Schmid, S. M. (2011). Cenozoic granitoids in the Dinarides of southern Serbia: Age of intrusion, isotope geochemistry, exhumation history and significance for the geodynamic evolution of the Balkan Peninsula. *International Journal of Earth Sciences*, *100*, 1181–1206. https://doi.org/10.1007/s00531-010-0599-x

Schmid, S. M., Bernoulli, D., Fügenschuh, B., Maţenco, L., Schefer, S., Schuster, R., et al. (2008). The Alpine-Carpathian-Dinaridic orogenic system: Correlation and evolution of tectonic units. *Swiss Journal of Geosciences*, *101*, 139–183. https://doi.org/10.1007/s00015-008-1247-3

Schmid, S. M., Fügenschuh, B., Kounov, A., Matenco, L., Nievergelt, P., Oberhänsli, R., et al. (2019). Tectonic units of the Alpine collision zone between Eastern Alps and Western Turkey. *Gondwana Research*, *78*, 308–374. https://doi.org/10.1016/j.gr.2019.07.005

Sherwood Lollar, B., Ballentine, C. J., & O'Nions, R. K. (1997). The fate of mantle-derived carbon in a continental sedimentary basin: Integration of C/He relationships and stable isotope signatures. *Geochimica et Cosmochimica Acta*, *61*, 2295–2307. https://doi.org/10.1016/S0016-7037(97)00083-5

Shimizu, A., Sumino, H., Nagao, K., Notsu, K., & Mitropoulos, P. (2005). Variation in noble gas isotopic composition of gas samples from the Aegean arc, Greece. *Journal of Volcanology and Geothermal Research*, *140*(4), 321–339. https://doi.org/10.1016/j.jvolgeores.2004.08.016

Sibson, R. H. (2013). Stress switching in subduction forearcs: Implications for overpressure containment and strength cycling on megathrusts. *Tectonophysics*, *600*, 142–152. https://doi.org/10.1016/j.tecto.2013.02.035

Sibson, R. H. (2020). Dual-driven fault failure in the lower seismogenic zone. *Bulletin of the Seismological Society of America*, *110*, 850–862. https://doi.org/10.1785/0120190190

Szocs, T., Rman, N., Suveges, M., Palcsu, L., Toth, G., & Lapanje, A. (2013). The application of isotope and chemical analyses in managing transboundary groundwater resources. *Applied Geochemistry*, *32*, 95–107. https://doi.org/10.1016/j.apgeochem.2012.10.006

Tamburello, G., Pondrelli, S., Chiodini, G., & Rouwet, D. (2018). Global-scale control of extensional tectonics on CO_2 earth degassing. *Nature Communication*, *9*, 4608. https://doi.org/10.1038/s41467-018-07087-z

Todorović, M., Štrbački, J., Ćuk, M., Andrijašević, J., Šišović, J., & Papić, P. (2016). Mineral and thermal waters of Serbia: Multivariate statistical approach to hydrochemical characterization. In P. Papic (Ed.), *Mineral and thermal waters of southeastern Europe*. *Environmental Earth Sciences* (pp. 81–95). Springer. https://doi.org/10.1007/978-3-319-25379-4_5

Torgersen, T. (1993). ^3He fluxes in extensional basins: Limits on the role of magmatism in extensional basins. *Journal of Geophysical Research*, *98*(B9), 16257–16269. https://doi.org/10.1029/93JB00891

Torgersen, T. (2010). Continental degassing flux of ^4He and its variability. *Geochemistry, Geophysics, Geosystems*, *11*, Q06002. https://doi.org/10.1029/2009GC002930

Torgersen, T., & O'Donnell, J. (1991). The degassing flux from the solid Earth-release by fracturing. *Geophysical Research Letters*, *18*, 951–954. https://doi.org/10.1029/91GL00915

Vaselli, O., Minissale, A., Tassi, F., Magro, G., Seghedi, I., Ioane, D., & Szakács, A. (2002). Ageochemical traverse across the Eastern Carpathians (Romania): Constraints on the origin and evolution of the mineral waters and gas discharge. *Chemical Geology*, *182*(2–4), 637–654. https://doi.org/10.1016/S0009-2541(01)00348-5

Weinlich, F. H., Bräuer, K., Kämpf, H., Strauch, G., Tesař, J., & Weise, S. M. (1999). An active subcontinental mantle volatile system in the western Eger rift, central Europe: Gas flux, isotopic (He, C, and N) and compositional fingerprints. *Geochimica et Cosmochimica Acta*, *63*, 3653–3671. https://doi.org/10.1016/S0016-7037(99)00187-8

Zelić, M., Agostini, S., Marroni, M., Pandolfi, L., & Tonarini, S. (2010). Geological and geochemical features of the Kopaonik intrusive complex (Vardar zone, Serbia). *Ofioliti*, *35*, 33–47.